ORIGINAL PAPER

Calcite twinning constraints on paleostress patterns and tectonic evolution of the Zagros hinterland: the Sargaz complex, Sanandaj–Sirjan zone, SE Iran

SH. Shafiei · S. A. Alavi · M. Mohajjel

Abstract Based on analyses of calcite twins, we constrain the tectonic history of the Paleozoic Sargaz complex within the SE part of the Sanandaj–Sirjan zone (hinterland domain of the Zagros orogen), SE Iran. The mean width of measured calcite twins was 1.97 μm, corresponding to the width of type II twins; variations in twin width with twin density indicate that calcite twinning in the study area occurred at temperatures of between 170 and 200°C. These results support the interpretation that the twins developed at a shallower depth and lower temperature than those of greenschist facies metamorphism recorded in this complex, and that twinning is therefore mainly a late, post-metamorphic deformation process. The c-axis fabrics of the studied samples are monoclinic, consisting of an intense point maximum located slightly anticlockwise of the normal to the shear plane; this asymmetry indicates non-coaxial deformation and a dextral component of shear in the thrust zones. The geometric relationship between stress axes and bedding reveals that the reconstructed stress tensors mainly post-date F_1-folding. Compressional stress axes are oriented NE–SW. This compressional stress was probably related to the (oblique) subduction of the Neotethys beneath Central Iran by Middle Triassic–Jurassic times, during the Cimmerian orogeny.

Introduction

The Zagros orogen originated from the closure of the Neotethys following the complete consumption of oceanic crust at a NE-dipping subduction zone below central Iran and subsequent Cretaceous continental collision between the Afro–Arabian and Iranian continental fragments. This orogenic belt consists of the following four parallel tectonic zones (from NE to SW): (1) the Mesopotamian–Persian Gulf foreland basin, (2) the Zagros Fold–Thrust belt that from SW to NE suddivided into three units: (a) the Zagros simply folded belt (Falcon 1967), which consist of ca.13–14 km of shelf deposits of Permo-Triassic to late Cretaceous/Paleocene age similar to those of Arabia followed by a more complex pattern of synorogenic sedimentation up to the recent Pliocene (Berberian and King 1981; Sengor et al. 1988), (b) a crush zone (or High Zagros) with imbricated tectonic slices comprising Mesozoic limestone, radiolarites, obducted ophiolite remnants and Eocene volcanics and flysch, which are all thrusted onto the Zagros fold belt, and (c) the Zagros fault, with the Main Zagros Thrust separating the Zagros domains from the internal zone. (Berberian and King 1981; Alavi 1994), (3) the Sanandaj–Sirjan metamorphic zone (SSMZ; Stocklin 1968), (4) the Urumieh–DokhtarMagmatic assemblage (UDMA; Schroder 1944). Two major parallel domains

SH. Shafiei (✉)
Department of Mining Engineering, College of Engineering,
Shahid Bahonar University of Kerman,
P.O. Box 76135-133, Kerman, IR, Iran
e-mail: shafiei_shahram@mail.uk.ac.ir

S. A. Alavi
Department of Geology, Faculty of Earth Sciences,
University of Shahid Beheshti,
P.O. Box 1983963113, Tehran, IR, Iran

M. Mohajjel
Deparment of Geology, Faculty of Basic Sciences,
University of Tarbiat Modares,
P.O. Box 14155-175, Tehran, IR, Iran

of the SSMZ and UDMA, to the northeast of the Main Zagros Thrust, are presumed to be the result of a northeast-dipping subduction process of Neo-Tethyan oceanic crust beneath Iranian continental active margin (Berberian and King 1981). The Sanandaj–Sirjan metamorphic zone extends for 1,500 km along strike from Sanandaj in the NW to Sirjan in the SE. The rocks in this zone are the most highly deformed and share the NW-SE trend of its structures. In the Golpayegan area, Sanandaj-Sirjan metamorphic zone can be subdivided into two parts (Eftekharnejad 1981; Ghasemi and Talbot 2006; Fig. 1): (1) the northern part (north SSMZ), deformed in the Jurassic-Early cretaceous, contains many intrusive felsic rocks (such as the Alvand, Brojerd, Arak, and Malayer plutons). Evidence for Jurassic–Early Cretaceous deformation and metamorphism is provided by unconformities in the marginal sub-zone and complexly deformed sub-zones in the Golpayegan area(Mohajjel et al. 2003). (2) The Southern part (South SSMZ) consists of both Paleozoic strata that formed in an epicratonic setting and a Carboniferous–Permian mafic and ultramafic complex (253–279 Ma; Ghasemi 2001). The Paleozoic units were deformed and metamorphosed during the Early–Cimmerain orogeny in the late Triassic. Structures associated with Early Cim-

merian orogenic phase characterized by development of intense folding with south-southwest vergence and low grade greenschist metamorphism. The Early Cimmerian deformation which developed in the southern Iranian margin suggest that this margin acted at that time as an active margin. (Berberian and King 1981; Mohajjel et al. 2003; Shafiei 2007; Sheikholeslami et al. 2008). Polyphase deformation structures of the Sanandaj–Sirjan metamorphic zone are consistent with dextral transpressional deformation, which is related to the oblique convergence between the African–Arabian continent and the Iranian microcontinent (Mohajjel and Fergusson 2000; Sarkarinejad and Azizi 2008; Sarkarinejad et al. 2008). This dextral transcurrent component resulting from the existing of an oblique component in the subduction zone (Shafiei 2007; Sheikholeslami et al. 2008)

The main purpose of the present paper is to use analyses of calcite twinning to constrain the tectonic history of the hinterland of the Zagros orogen by reconstructing the paleostress fields and the depth at which deformation occurred in the Sargaz complex, SE Sanandaj–Sirjan metamorphic zone. Few comparable studies have been undertaken in Iran, and in this respect the present work will complement a recent study of late Neogene Arabia–Eurasia collisional stresses based on calcite twinning in the Zagros (Lacombe et al. 2007) by providing constraints on the pre-collisional tectonic history of the Zagros hinterland.

Geological setting of the study area

In the South SSMZ, Paleozoic strata subdivided into six syntectonic regional metamorphic complexes of varying metamorphic grade and age, all subsequently overlain by non-metamorphosed Early Jurassic basal conglomerates (that contain metamorphic clasts) and volcanic–detrital rocks. These complexes have been traced continuously from Hajiabad in the SE to Neyriz in the NW (Berberian 1976), and are each divided into the following three metamorphic units (from top to bottom): (1) upper complex (low grade), (2) middle complex (low to medium grade), and (3) lower complex (high grade). The conventional K/Ar radiometric age of a single sample of Zarab kyanite-sillimanite schist collected from the Neyriz area (Watters and Sabzehi 1970) is 404±8 Ma; i.e., the Silurian–Devonian boundary. Sections of the middle complex yield poorly preserved fragments of crinoids stems, several corals, and a single bryozoa, while Devonian pollen and spores have been reported from carbonaceous black schist (Berberian 1976).

The stratigraphic units in the present study area, which extends from longitude 57°21′-57°3′ and latitude 28°10′-28°15′ (Fig. 1), consist of the Paleozoic Abshour and
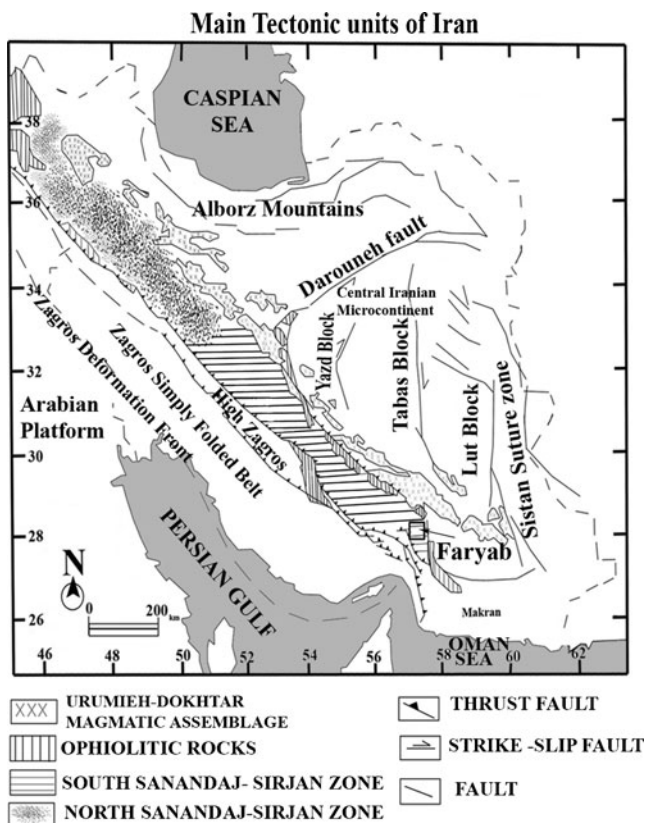

Fig. 1 Tectonic zones of the Zagros orogen in western Iran and location of the Faryab area in the southeast part of the Sanandaj–Sirjan metamorphic zone

Sargaz complexes (middle complex; Sabzehi 1974). The Abshour complex comprises marbles, meta-basaltic lava, and meta-dolomites, while the Sargaz complex, which rests conformably upon the Abshour complex, consists of the following units: (1) interbedded marbles and calcschists, (2) metamorphosed volcanic rocks, and (3) quartz- and muscovite-rich schists. This sequence is unconformably overlain by lower–middle Jurassic conglomerates and sandstones (Fig. 2).

Some authors have interpreted these metamorphic complexes as Precambrian basement rocks (e.g., Stocklin 1968); however, others have proposed that Early Cimmerian tectonics were responsible for their syntectonic regional metamorphism (Berberian 1972, 1973, 1976; Hushmandzadeh et al. 1972; Majidi 1972, 1974; Sabzehi and Berberian 1972; Berberian and Nogol 1974; Sabzehi 1974). The Faryab area within the SE Sanandaj–Sirjan metamorphic zone (internal part of the Zagros belt) records twofold events. F_1-folding have appeared in gently inclined to recumbent style and include mesoscopic, macroscopic folds and axial planar schistosity. This
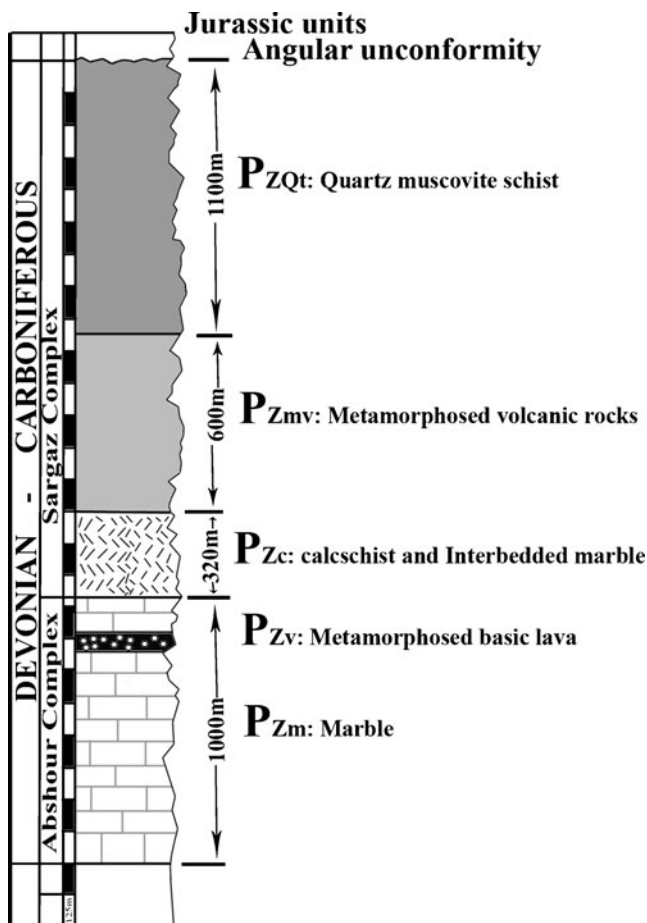
generation is well documented in the Sargaz and thin units of Abshour complexes. Axial planar schistosity is commonly parallel to bedding (Fig. 3a,b). The axial planes of F_1-folds dip 10-30° to the NE and their axes plunge gently to the W. F_1-folds formed by flexural flow, and thrust faults developed along overturned limbs. Formation of thrust is a result of differential flow in a ductile mass forming F_1-folds, then shearing out of common limb between the antiform and synform forming these thrusts. At the southern edge of the central domain, these faults displaced large slices of calcschists and interbedded marbles. Fig. 3c, e). F_2 folds, which co-axially refold F_1-folds, are well-exposed in the Pasefid, Zartorosht, and Zehmakan anticlines. F_2-folds axes are variable in orientation, trending in the range between S45W and N80W (Fig. 3f). In the eastern and central domains (Fig. 4), two outcrops show interference patterns of Z on S, M on S, and S on S, indicating coaxial refolding of F_1 by F_2 (hook shape interference pattern; Fig. 3g–j). The orientations of F_1 and F_2 fold axes are consistent with this pattern of refolding (Shafiei 2007).

Sampling strategy and measurement

To constrain the stress and kinematic history of the Sanandaj–Sirjan metamorphic zone in the present study area based on analyses of calcite twins, six oriented samples from F_1-folds in the south of Zartorosht Au-Index in the central domain and 13 samples from thrust shear zones were collected from calcschists within the Sargaz complex. For each sample, measurements (c-axis, orientation of twin lamellae, number and width of twins, and grain width) were made using a U-stage from matrix in the host rocks. About 50 grains were measured in two perpendicular thin sections: one oriented normal to bedding and parallel to its strike, and the other normal to bedding and parallel to its dip (Fig. 4, Table 1). Our measurements show that the 60% of calcite grains appear with two twin sets (Fig. 7) while 40% display a single twin set.

Results

Temperature of calcite twinning deformation

The width of calcite twins is an important parameter in constraining the temperature of deformation. The range in twin widths within samples from the Faryab area is from 1 to 3.8 μm (mean, 1.97 μm) indicating deformation under a thick twin (type II) regime (Fig. 5; Burkhard 1993). The range of twin densities is between 24.8 and 72.7(number/millimetre, Table 1). According to Ferrill et al. (2004)

Fig. 2 Stratigraphic column of the Faryab area showing the approximate stratigraphic thicknesses of units

Fig. 3 **a** Gentle inclined folding in thin layer units of Abshour complex near Pasefid and **b** Formation of gentle inclined folds under flexural flow conditions in calcschists unit of Sargaz complex (SW of Zartorosht Au index). In this mechanism, hinge collapsed (HC) and axial surface schistosity have been developed. **c**, **d** Formation of thrust by differential flow in a ductile mass forming a fold , then shearing out of common limb between the antiform and synform forming a thrust. **e** At the southern edge of the central domain, thrust faults displaced large slices of calcschists and interbedded marbles. **f** Pasefide anticline F_2-fold in marble of Abshour complex. **g** Outcrop of refolding F_1-fold by Z-type F_2-fold. **h**, **i**, **j**) Z on S, M on S and S on S patterns in outcrop of interference pattern in central domain (C.I.P in Fig. 4)
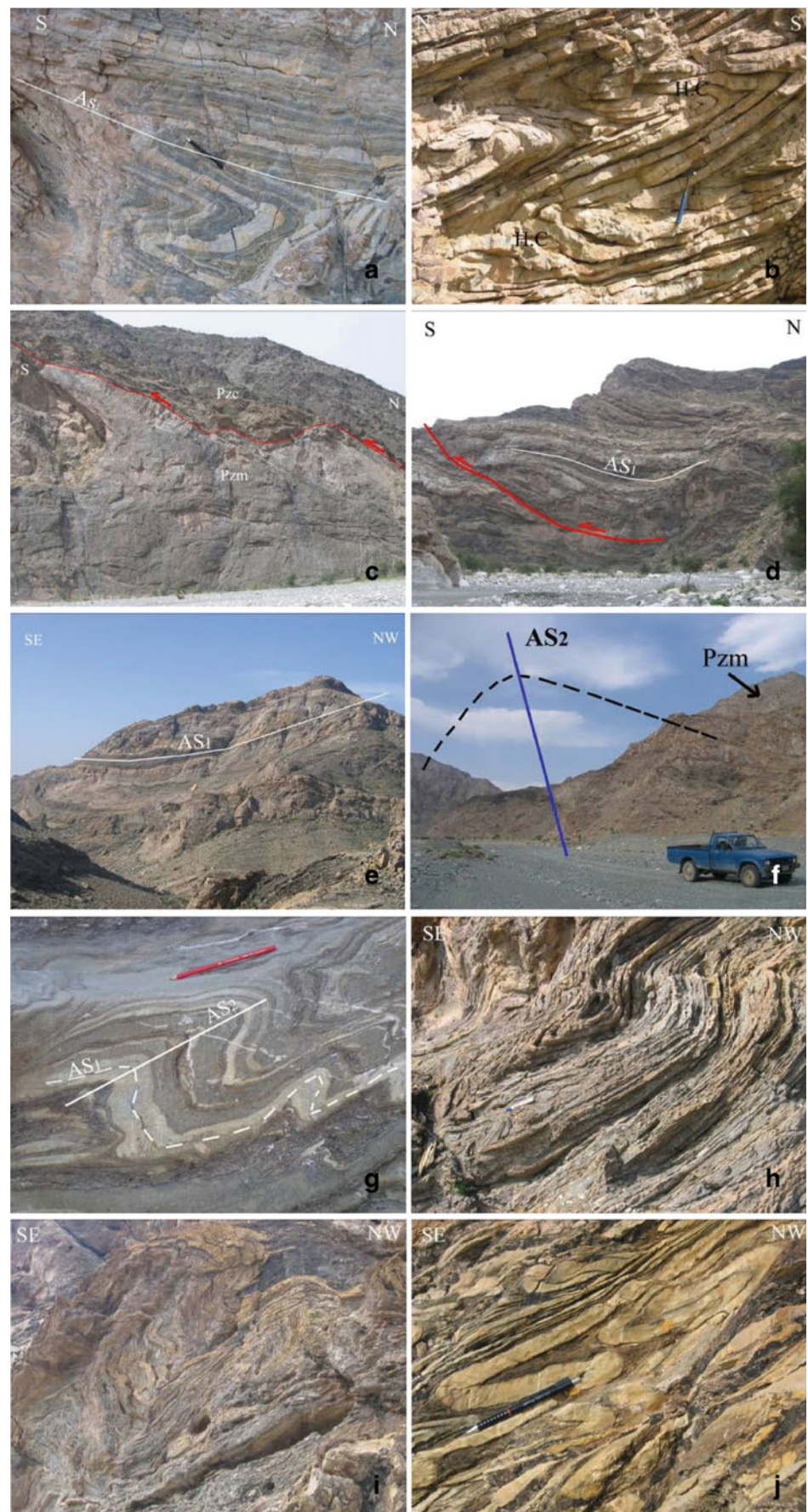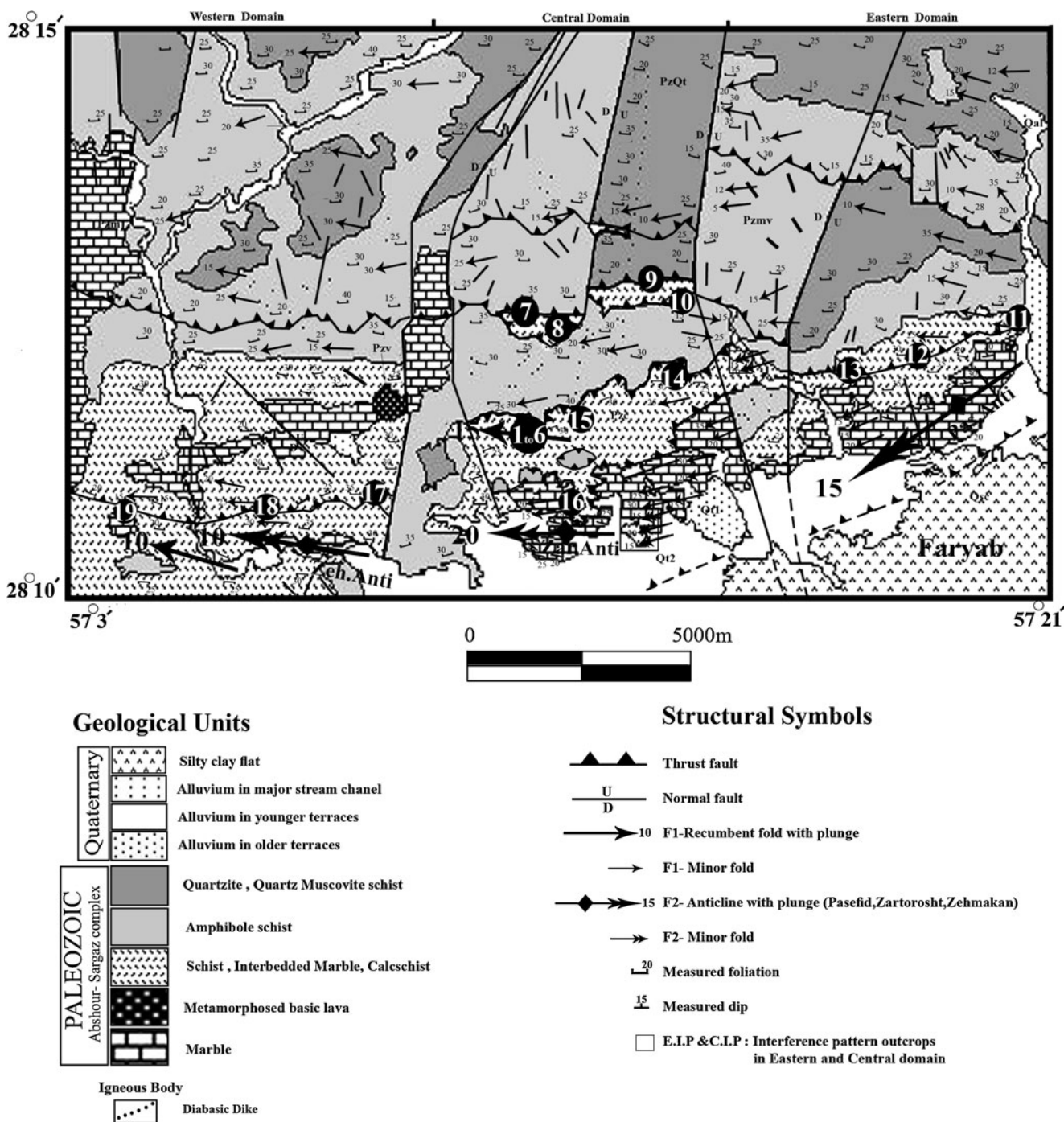
Fig. 4 Structural map of the Faryab area. *1–6* the locations of samples (*black circle* with number of sample) were collected from F1-folding; *7–19* are the locations of samples were collected from thrust shear zones

diagram of twin width versus twin density, the temperature of deformation for the present samples is 170–200°C and the twinning strain never exceeds a few percents (Fig. 6).

These results indicate that the temperature of twin formation is inconsistent with the greenschist facies temperature and pressure conditions recorded in the

Faryab area. Groshong et al. (1984) already reported that twinning does not occur at peak metamorphism but rather postdates metamorphism. In the present study, the mean twin width, the high percentage of type II twins, and estimates of deformation temperatures all indicate that twinning occurred relatively late, as a post-metamorphic deformation process.

Table 1 Mean number of twins, grain size, and twin density for each of the samples used to determine differential stress

Sample	Host or vein or both	Strike (dip) of foliation	Mean of no twin per grain	Mean of grain size (microns)	Twin intensity (no/mm)	Differential stress (MPa; Rowe and Rutter 1990)
1	Host	E-W (15 S)	23.8	385	60.7	205
2	Host	N85W (10SW)	10.1	230	43.2	184
3	Host	E-W (10 S)	17.8	390	36.8	198
4	Host	E-W (25 S)	12.3	250	49.4	193
5	Host	N70W (20SW)	18.35	360	50.3	195
6	Host	N85W (15SW)	15.7	215	71.4	196
7	Host	E-W (35 N)	11.8	500	24.8	371
8	Host	E-W (30 N)	11.2	416	26.8	149
9	Host	N70W (25NE)	16.8	250	64.8	214
10	Host	E-W (20 N)	15.1	200	64.7	214
11	Host	N80E (25NW)	11.4	300	38	175
12	Host	E-W (30 N)	14.5	225	64	213
13	Host	N80W (20NE)	9.9	245	48	195
14	Host	E-W (30 S)	15.4	360	42.6	183
15	Host	N80-W (30SW)	12	270	43.9	186
16	Host	E-W (30 S)	10.6	160	64	214
17	Host	E-W (40 N)	18.2	390	47.4	191
18	Host	N80E (25NW)	18.9	255	72.2	222
19	Host	E-W (20 N)	17.7	320	54.5	202

Kinematic interpretation of calcite fabrics

Wenk et al. (1987) proposed a subdivision of c-axes fabrics of calcite into low-temperature (LT) and high-temperature (HT) types. LT fabrics correspond to those obtained experimentally that show twinning (with minor intracrystalline slip) as the dominant deformation mechanism, whereas HT fabrics correspond to the experimental fabrics for which intracrystal-

line slip is dominant. LT fabrics have a single point maximum oriented approximately parallel to the principal stress axes and oblique to the shear plane; consequently, the orientation of this maximum could be used as a shear sense indicator or a measure of the degree of non-coaxiality of the deformation.

LT fabrics are divided into LT pure shear and LT simple shear. LT pure shear fabrics have a single point maximum oriented normal to the shear plane. The LT simple shear
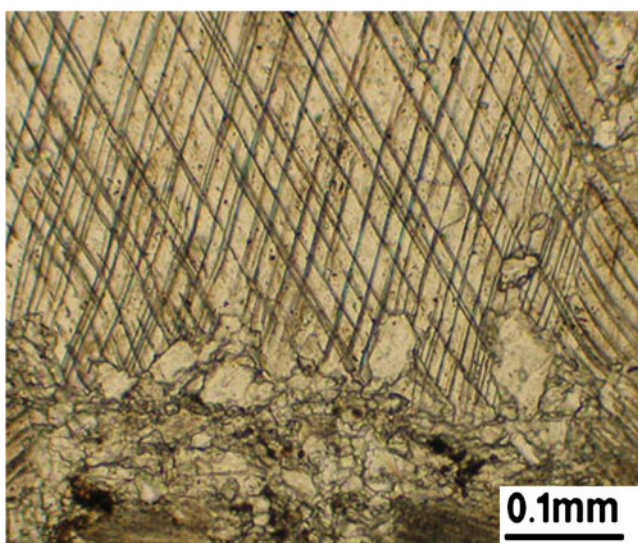

Fig. 5 Colour microphotograph of Type II twins in calcite from the Faryab area (width of view, 2 mm; PPL)
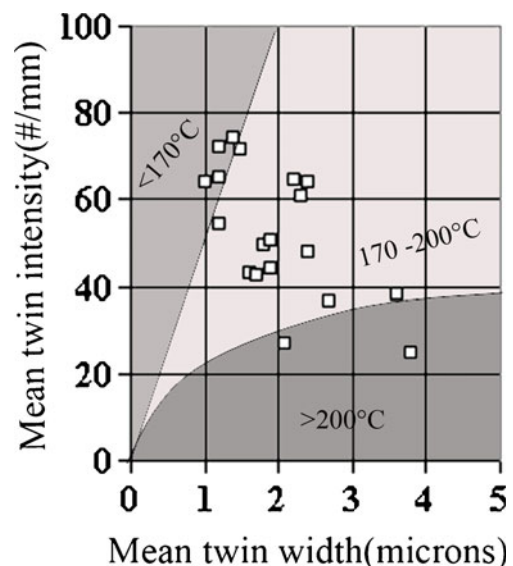

Fig. 6 Plot of mean twin intensity versus mean twin width in samples from the Faryab area (adapted from Ferrill et al. 2004)

fabrics are similar to the LT pure shear fabrics, but rotated counter to the sense of shear. In LT fabrics, c-axes are subhorizontal to gently plunging (Lafrance 1994). These fabrics show a girdle with one or two unequal peripheral maxima with monoclinic symmetry.

Figure 7 show plots of optic c-axis orientations of from samples 1 to 19. The calcite c-axes fabrics recognised in samples 1-6 reflects a LT pure shear fabrics conditions. In these samples concentrations of c-axes show a point maxima normal to the foliation, whereas in the samples related to thrusts shear zones (samples 7–19), concentrations of c-axes are very intense point maxima located anticlockwise of the normal to the shear plane and reflect a LT simple shear fabrics.

According to deformation style in the Sargaz complex, appearance of two twin sets in calcite grains is likely the result of the F_2-folding phase. F_2-folding is a post-metamorphic event consistent with NE-SW shortening that was in continuation and co-axial with F1-folding. Consequently, calcite c-axes fabric in the samples 1-6 rather reflect the final phase of deformation at decreasing temperatures and do not reflect F_1-folding conditions. This obliquity or asymmetry in the LT fabrics indicates non-coaxial deformation and a component of dextral shear along the thrust zones (Figs. 7, 8; Lafrance 1994). Based on Turner and Weiss (1963), the orientations of c-axes in samples1-6 from the Faryab area indicate post or syn-tectonic (post-F_1-folding or syn F_2-folding) twinning.

Paleostress orientations from calcite twins

The direction and/or magnitude of paleostress can usually be determined by analysing the fabrics of certain minerals


Fig. 7 Calcite twinning data, including compression and tension axes and c-axes (lower-hemisphere, equal-area stereographic projections, contour levels 1%). Foliation plane illustrated in compressive diagrams
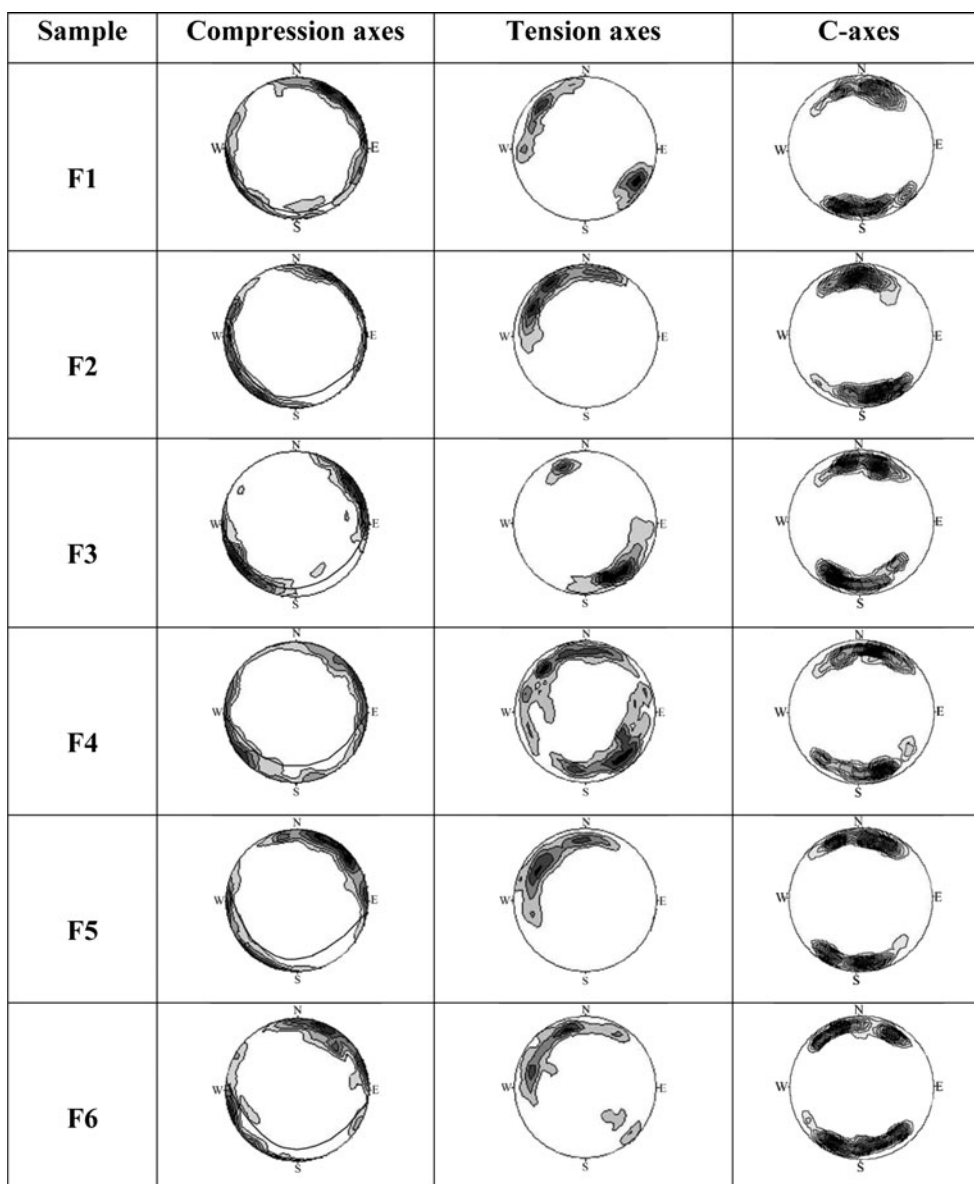
(e.g., Tullis 1980). Such information plays an important role in constraining the stress history of orogens and forelands (e.g., Lacombe 2001). Mechanical twinning is commonly observed in calcite deformed at low pressure (P) and temperature (T) (Turner 1953; Rowe and Rutter 1990; Burkhard 1993; Newman 1994; Ferrill 1998). The orientations of calcite twin lamellae can be used to determine the direction and sometimes the magnitude of paleostresses at the time of deformation. Several methods of strain and stress analysis have been developed based on calcite e-twin data (e.g., Turner 1953, 1962; Weiss 1954; Turner and Weiss 1963; Spang 1972; Laurent et al. 1981, 1990, 2000; Groshong 1972; Groshong et al. 1984; Rowe and Rutter 1990; Ferrill 1991, 1998; Lacombe and Laurent 1992, 1996; Burkhard 1993; Evans and Groshong 1994; Newman 1994). Some of these methods allow either the complete

(principal stress orientations and magnitudes) or partial (principal stress orientations only) determination of stress tensors (e.g., Lacombe 2001, 2007): others provide only paleo-differential stress magnitudes based on twin density or the percentage of carbonate grains with one, two, or three twin sets (e.g., Jamison and Spang 1976; Rowe and Rutter 1990). The application of calcite twin analyses to the reconstruction of stress history has proved to be highly successful in many tectonic settings, including forelands (e.g., Sevier and Appalachian: Craddock et al. 1993; van der Pluijm et al. 1997, Northern Pyrenean: Rocher et al. 2000, Southern Pyrenean: Gonzales-Casado and Garcia-Cuevas 1999, Taiwan: Lacombe et al. 1993; Rocher et al. 1996, and the Zagros: Lacombe et al. 2007), and hinterlands of orogens (e.g., Alps: Pfiffner 1982; Cantabrian zone: Rowe and Rutter 1990).

Fig. 7 (continued)

| Sample	Compression axes	Tension axes	C-axes
F7			
F8			
F9			
F10			
F11			
F12			
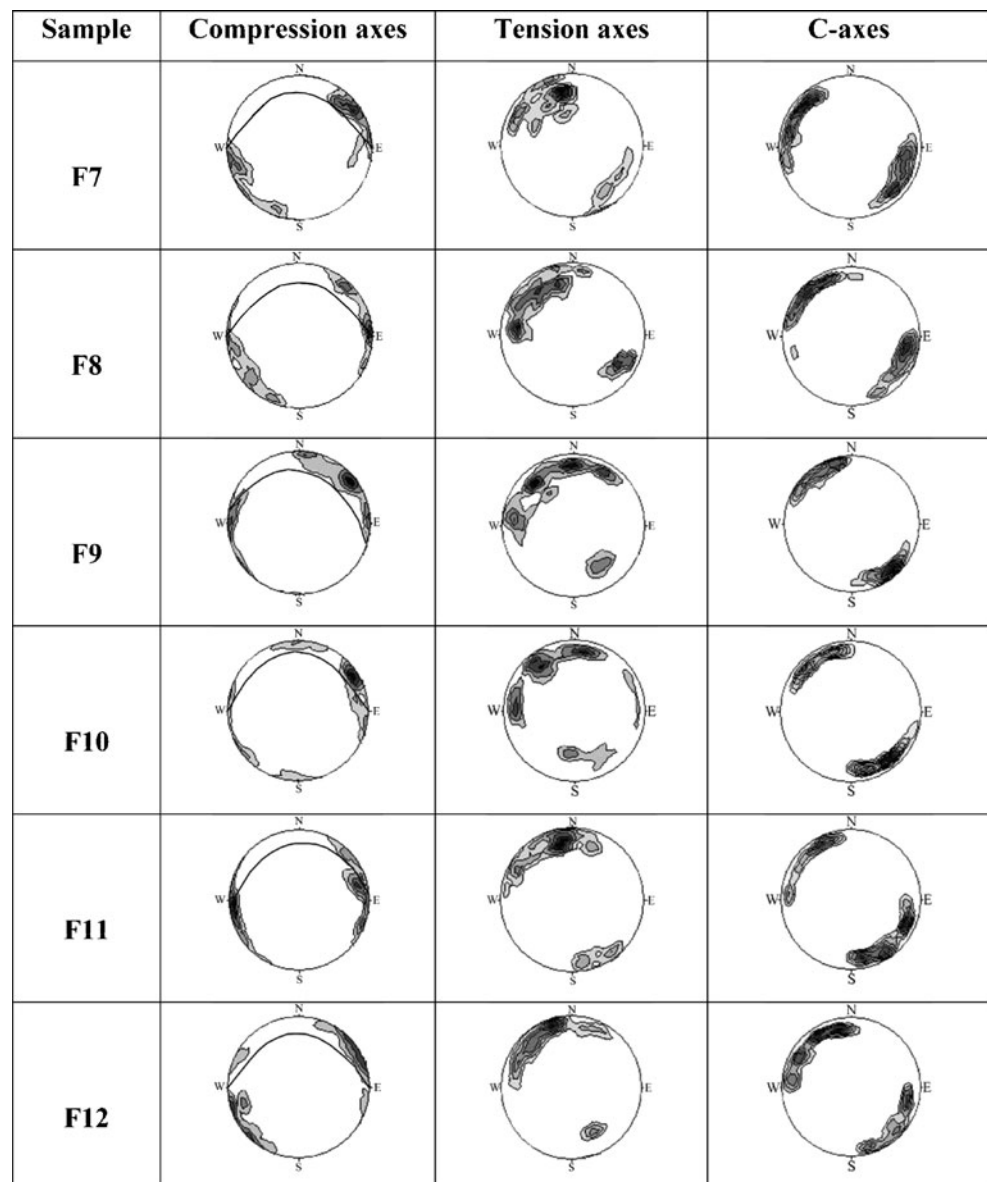
The orientations of calcite twin lamellae can be used to determine the orientation of the paleostress field at the time of deformation. Methods of stress analysis based on calcite twins share the fundamental assumption that the measured twins formed in a homogeneous stress field and were not passively rotated after formation. Stress directions are defined in terms of compression and tension directions as first introduced by Turner (1953). Among the limitations of this method is that it applies to monophase calcite aggregates and that the analysis of calcite twins in term of stress is dependent on the occurrence of a preferred *c*-axis fabric.

The consistent regional contouring pattern maxima of optic *c*-axis orientation in our samples show that there was a preferred orientation of calcite when it was later twinned at lower temperature. We however perform the twin analysis in order to evaluate the consistency of the kinematic interpretation of *c*-axis fabrics with stress results
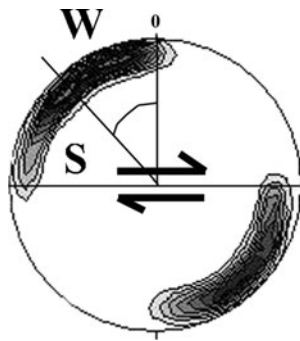
Fig. 7 (continued)
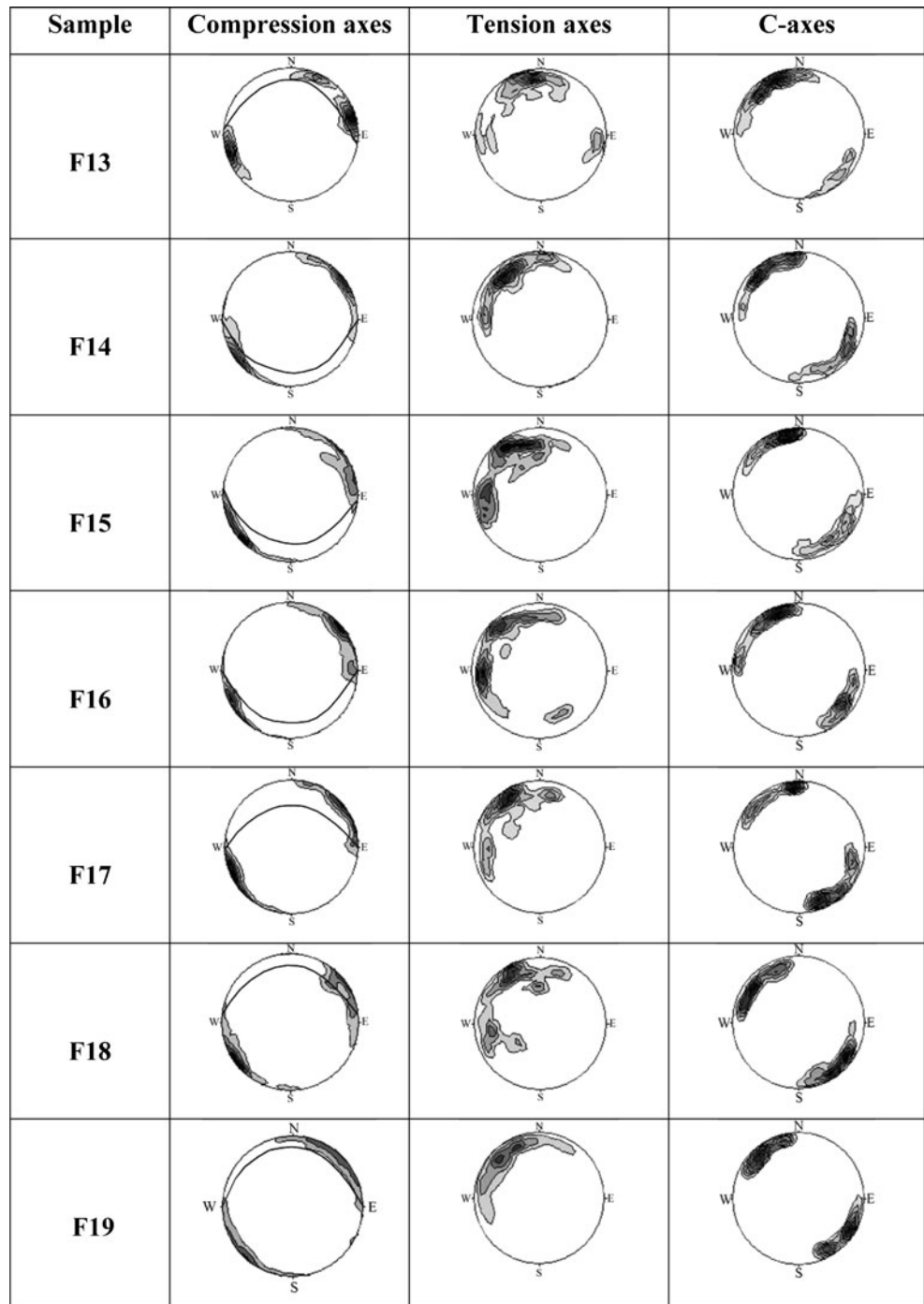
Fig. 8 Assymetrical concentration of calcite *c*-axis fabrics in the samples from thrust shear zones (samples *7*–*19*). This obliquity or asymmetry in these fabrics indicates non-coaxial deformation and a component of dextral shear along the thrust zones. *w* is angle between the point maximum and normal to shear plane is oriented anticlockwise of the shear plane(S) in thrust shear zones

derived from later calcite twinning. We used the Calctstress Software (Shelly 1989) to compute the direction of the main compressional and tensional vectors. This software considers U-stage data of the orientation of calcite *c*-axes and e-twin lamellae, and calculates the compression and tension directions for each *c*-axis/e-twin lamellae pair. Data were collected in separate files for *c*-axes, e-twin lamellae, compression directions, and tension directions in a form suitable for direct use in stereographic projection software. If a grain of calcite may contain two or three e-twin lamellae, the *c*-axis reading for those grains will be repeated two or three times in the output data (Shelly 1989). Figure 7 shows the orientation of *c*-axes and calculated compression and tension directions.

The orientation of the principal stress axes were obtained by using the orientation measurements of the twin planes and *c*-axes to calculate the compression and tension directions for each measured grain and then by contouring the results obtained from all the grains measured in the given samples on the an equal stereographic projection (Turner 1953, 1962; Weiss 1954; Pfiffner and Burkhard 1987).

The stress system deduced from *c*-axes and twin planes data is monoclinic, with σ_3 coinciding with the maximum for tension axes and σ_1 plotting close to the maximum for compression axes. The compression axes (σ_1) trend NE–SW, with shallow plunges (7-19°); the tension axes (σ_3) trend NW–SE, with moderate plunges (12-54°). Two stress axes (σ_1 and σ_3) are subhorizontal and σ_2 axis is subvertical. The orientations of the mean principal stress axes are plotted on cross-sections across the eastern (A–A′), central (B–B′), and western (C–C′) domains. Interestingly, geometric relationship between compressional stress axes and bedding indicate that twinning postdates F$_1$-folding (Figs. 9 and 10). This is in good agreement with the thin-twin regime indicating that twinning occurred during the latest stage of deformation. This also show that layer-

parallel shortening, commonly (although not always) recorded in thrust belts (e.g., Craddock et al. 1993) has not been either recorded or preserved. Although the calculated tensors are rather of strike-slip type, the trend of the maximum compressional stress axes σ_1 is consistent with the kinematics of thrusts and F$_2$-folds, which suggests a kinematic continuum through time. Interestingly, there is no obvious record by twinning of late normal faulting as shown in sections of Fig. 10; this may be related either to the heterogeneous character of late brittle faulting or to calcite strain hardening.

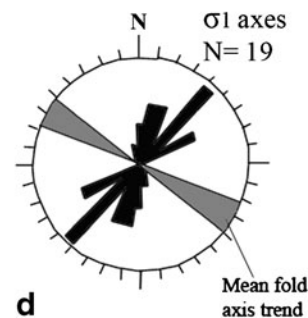Paleodifferential stress magnitudes from calcite twins

Calcite twin data from the Sargaz complex were also used to constrain the magnitudes of differential stress. In the case of calcite twinning paleopiezometry, it is assumed that stress is homogeneously distributed at the grain scale in natural rocks; however, this is probably a rare limiting case. The aim of paleopiezometry is to extrapolate the measured stresses to a regional, kilometric scale (Burkhard 1993).

The most widely used calcite-based paleopiezometric technique is that of Jamison and Spang (1976). Its basis is as follows: in a sample without any preferred crystallographic orientation, the relative percentages of grains twinned on 0, 1, 2, or 3 twin plane(s) depend on the applied (σ_1-σ_3) value. Since this relationship has been experimentally calibrated, knowing these relative percentages in a sample and under the hypothesis of a constant critical shear stress value for twinning, the order of magnitude of (σ_1-σ_3) can be estimated. Among the limitations of this method is that it does not take into account the grain size dependence of twinning, does not check the mutual compatibility of measured twin systems, and therefore should only apply to monophase samples and is valid only if the stress tensor is of revolution.

Jamison and Spang (1976) technique also requires the assumption of a constant value for the critical resolved shear stress for twinning, t_c. A t_c value of 10 MPa was originally determined for large single crystals of calcite (Turner 1953; Friedman 1976; Tullis 1980). Rutter (1995) suggested that a t_c value of 10 MPa is not universal; however, Lacombe and Laurent (1996) analysed experimentally deformed coarse-grained Bathonian Limestone (deformed at room temperature) and Carrara marble (deformed at 280 and 400°C), and found that values of maximum differential stress estimated by assuming a t_c value of 10 MPa were consistent with differential stresses actually applied during the experiments. On this basis, the authors concluded that the t_c value of 10 MPa commonly adopted for estimates of differential stress is reasonable (Ferrill 1998). Lacombe (2001, 2007) have refined these
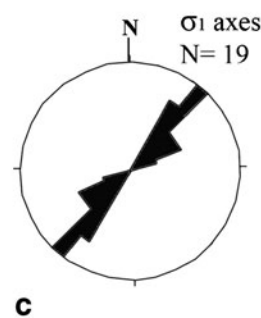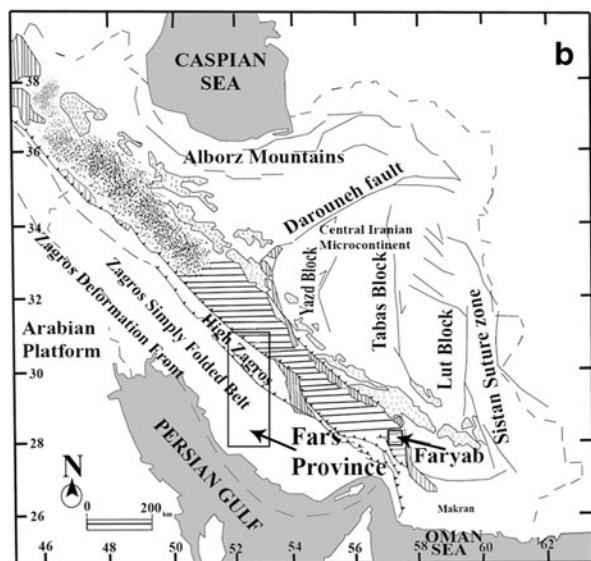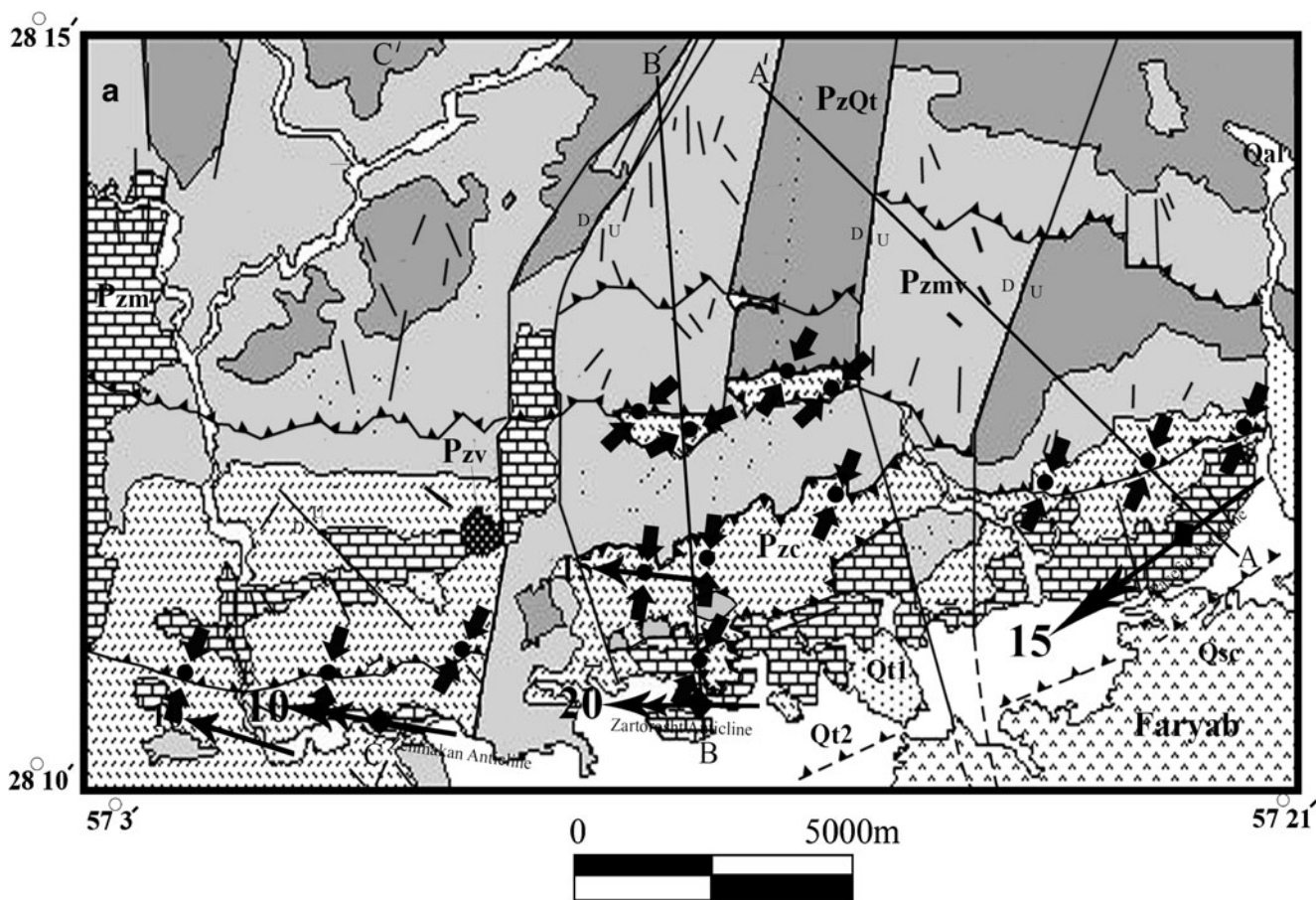
Fig. 9 **a** Orientations of σ₁ axes in the Faryab area for each sampling location in the Faryab area. **b** Two areas in which the compressional stress orientations were constrained based on analyses of calcite twins: the Faryab area (Sanandaj–Sirjan zone) and the Fars province, comprising the Zagros Simply folded belt and southern Iranian Plateau. **c, d** Rose diagram of local σ₁ trends in the Faryab area (Shafiei 2007) and Zagros Simply folded belt (Lacombe et al. 2007).

In the Sanandaj-Sirjan metamorphic zone, Thrusts faults have a NW-SE trend with NE-SW vergence. In the East of faryab area, due to influence of Sabzevaran dextral Strike–slip fault (upper Cretaceuos), NW-SE trend rotated to the E-W. If we balance the E-W trend of Thrust faults to the NW-SE, it is concluded the stress direction deduced by calcite fabrics is consistent with dextral strike-slip component within thrust faults

Fig. 10 Types of principal
stress axes related to NE–SW
compression deduced from
analyses of calcite twins. **a**
Cross-section A–A′ in the
eastern domain, **b** cross-section
(B–B′) in the central domain,
and **c** cross-section (C–C′) in the
western domain (see Fig. 9 for
location of cross-sections). The
geometric relationship between
bedding and the principal stress
axes supports the interpretation
that the calculated stress tensors
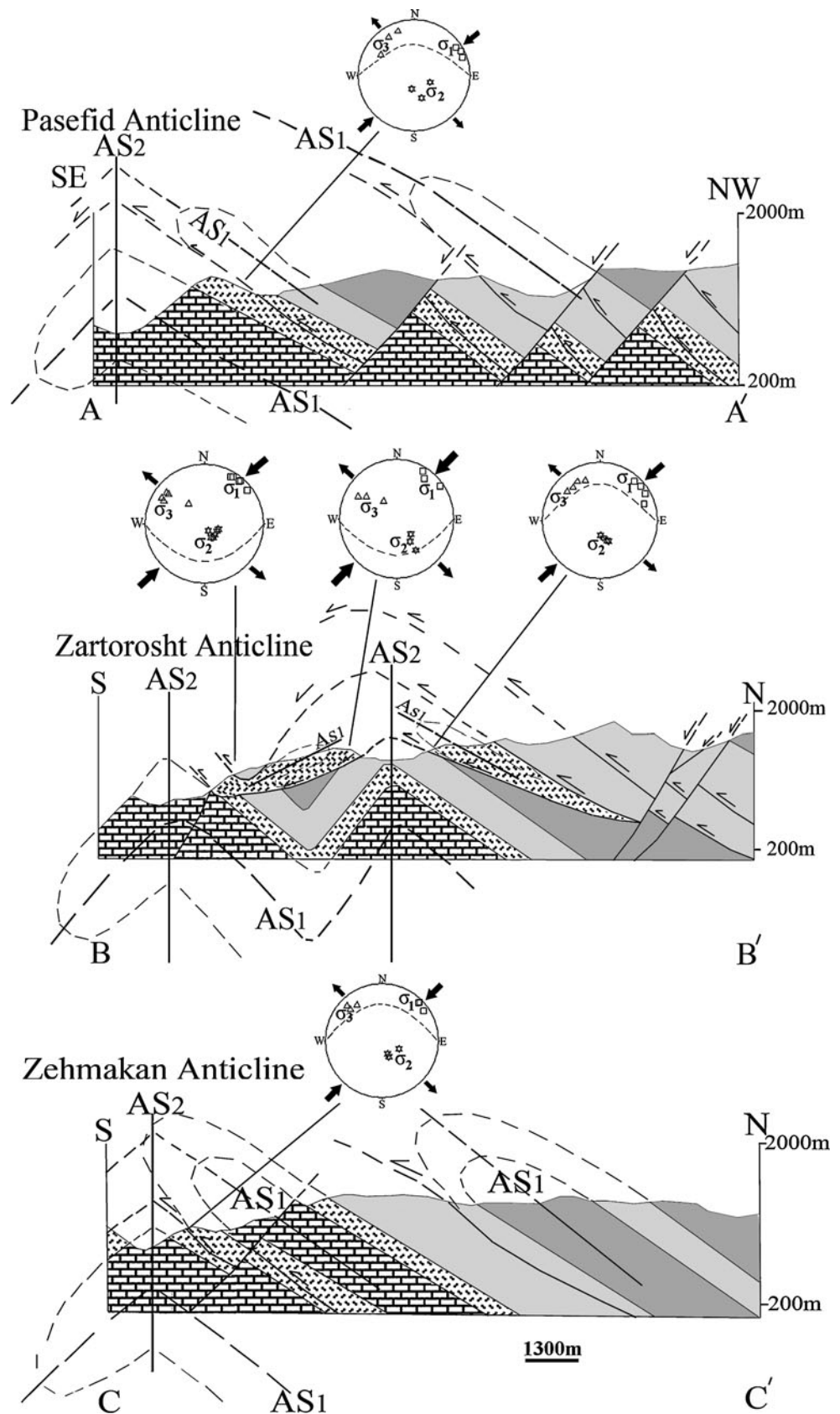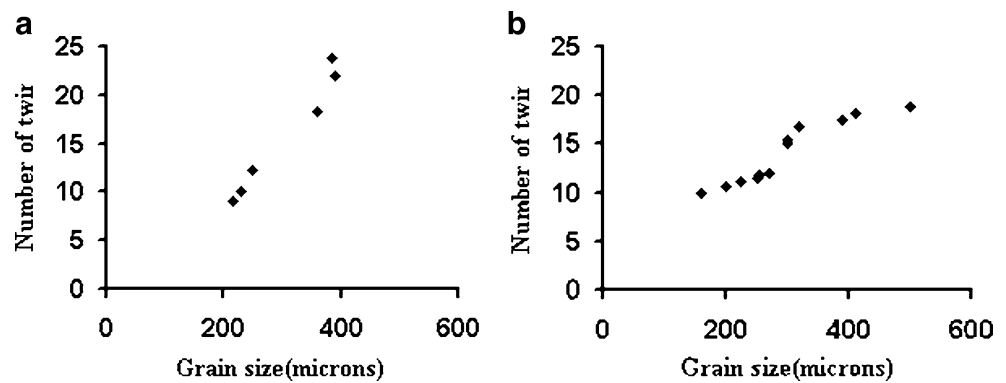post-date F_1-folding

Fig. 11 a, b Linear relationships between the number of twins and grain size for samples from the Faryab area associated with F_1-folding (a) and thrusting (b)

estimates and suggested a value of 10±4 MPa, depending on the mean grain size and internal twinning strain.

In the present study, differential stresses related to late twinning was calculated based on Rowe and Rutter (1990) method. The main parameter in this method is twin density (number of twins per millimetre). Twin density (D) is here defined as the rate of change in the number of lamellae of a given twin set with respect to grain diameter, measured normal to the trace of the twin lamellae (Rowe and Rutter 1990). The number of twins measured in the present study increases approximately linearly with grain size (Fig. 11). Twin density shows a linear relation with differential stress, but is independent on grain size (Rowe and Rutter 1990); accordingly, we also found an increase in twin density (intensity) with increasing differential stress (Fig. 12).

With increasing differential stress, progressively a larger number of grains occur in which all three e-planes are subjected to a sufficient component of shear stress for twinning to occur; consequently, the proportions of grains with none, one, two, or three twin sets can be regarded as a function of the magnitude of differential stress (Burkhard 1993). Based on $\sigma = -52 + 171.1 \log D$ and a standard error of 43 MPa (Rowe and Rutter 1990), values of differential stress calculated in the present study are about 195 MPa (Table 1).

Paleodepth of late twinning deformation

Lacombe (2001) reported a decrease in differential stresses from the hinterland to the foreland of orogens. In the foreland, the differential stresses decreased from 100 MPa close to the orogenic front to 10–20 MPa in the far foreland, mainly reflecting stress attenuation as a function of distance from the plate boundary (all of the foreland rocks were likely to have been deformed at similar depths). Although this effect may also apply at the scale of the entire orogenic system, the increase in differential stress from 10–20 MPa in the foreland to 200 MPa in the hinterland (Fig. 12) rather indicates an overall increase in differential stresses with depth, as rocks currently exposed at the surface in fold–thrust belts and metamorphic belts were deformed at much deeper crustal levels than foreland rocks during crustal wedging.

Three main stress–depth domains can be recognised in Fig. 12 (Lacombe 2001): the foreland domain, composed mainly of sedimentary rocks deformed at shallow depth (between 0 and 2 km) under differential stress values of between 5–10 and 40 MPa; the fold–thrust belt domain, composed of both sedimentary and weakly metamorphosed rocks deformed at depths of between 300 m and 4–5 km under differential stress values of between 30 and 140 MPa; and metamorphic rocks of the inner belt domain, deformed
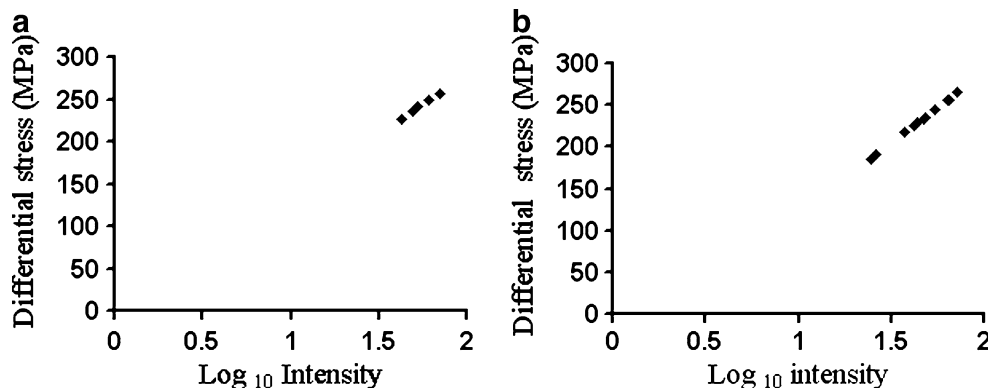

Fig. 12 a, b Differential stress plotted against the log number of twins per millimetre for Faryab samples associated with F_1-folding (a) and thrusting (b). The best-fit straight line is $\sigma = -52 + 171.1 \log D$ (Rowe and Rutter 1990)

at depths of between 5 and 15 km under differential stress values of between 50 and 200 MPa. This trend of increasing differential paleostress with depth supports the interpretation that most of the upper crust is probably at or near frictional equilibrium (Lacombe 2007), as also indicated by in situ stress measurements (Townend and Zoback 2000).

For given stress and pore pressure regimes, it is possible to predict the maximum differential stress based on the frictional-failure equilibrium hypothesis and to compare this prediction with observed values. For a favourably oriented pre-existing cohesionless fault plane, the condition of reactivation, which therefore applies to a critically stressed crust, can be written as follows (Jaeger and Cook 1969):

$$(\sigma_1 - P_f)/(\sigma_3 - P_f) = \left[(\mu^2 + 1)^{0.5} + \mu \right]^2$$

This equation can be used to predict differential stress as a function of depth in crust at frictional equilibrium. For compressional settings [i.e., the largest principal stress σ_1 is horizontal, such that the states of stress are of strike-slip (σ_2 vertical) or reverse-type (σ_3 vertical) regimes],

the following equations for strike-slip and reverse-type regimes have been considered:

$$\sigma_1 - \sigma_3 = 2\rho gz(\lambda - 1)\left(1 - \left[(\mu^2 + 1)^{0.5} + \mu \right]^2 \right)$$
$$/ \left(1 + \left[(\mu^2 + 1)^{0.5} + \mu \right]^2 \right) \text{ and } \sigma_1 - \sigma_3 = \rho gz(\lambda - 1)$$
$$\left(1 - \left[(\mu^2 + 1)^{0.5} + \mu \right]^2 \right)$$

where, $\lambda = P_f/\rho gz$. The value of λ is approximately 0.4 for hydrostatic conditions, 0.9 for near-lithostatic conditions, and exactly 0 for dry conditions. Figure 12 shows differential stress–depth curves that correspond to strike-slip and reverse faulting regimes for values of λ of 0.38 (hydrostatic) and 0 (dry) and for values of the friction coefficient μ of 0.6 and 0.9 (Lacombe 2007). Based on the differential stresses related to F1 folding and thrusting, and assuming that the crust is close to frictional equilibrium, the depth of deformation for the samples analysed in the present study is estimated to be around 7–8 (±1) km. These estimates of the magnitudes of differential stresses and depth of deformation are consistent with the tectonic setting of deformation of the Sargaz complex in the inner belt of the Zagros orogen (Fig. 13).

Fig. 13 Values of differential stress derived from the relationship between paleopiezometry and depth (log–log). Dashed lines represent the stress–depth relationship predicted by Coulomb frictional-failure theory for coefficients of friction μ of 0.6 and 0.9, pore pressures of 0 (λ=0) and hydrostatic (λ=0.38), and various tectonic regimes (SS, strike slip; R, reverse) (adapted from Lacombe 2007). Differential stress and depth of deformation are reported for the Faryab area
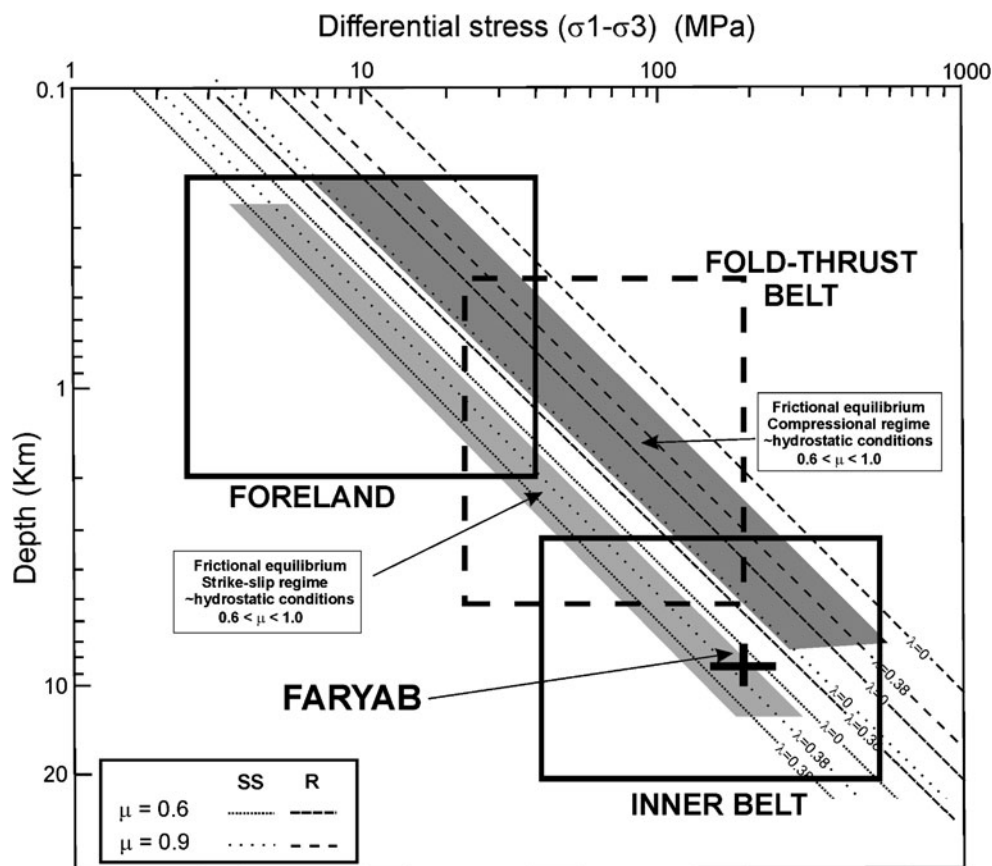
For an Andersonian stress regime, the principal stress is vertical and equal to the effective weight of overburden ($\rho gz - P_f$), where ρ is the average density of overburden, g is the acceleration of gravity, z is depth, and P_f is fluid pressure. Evaluating the weight of overburden requires an estimate of the paleo-depth at the time of the tectonic event, i.e., 7–8 km in the present case. Given that the pore fluid pressure at the time of deformation cannot be determined, we adopt hydrostatic conditions as the most realistic conditions of fluid pressure (Lacombe 2001, 2007). In the present study, the orientation of the principal stress axes (Fig. 8) indicates that $\sigma_2 = \sigma_v = (\rho - \rho_e)gz$, with $\rho = 2,700$ kg/m^3 (average density of overburden) and $\rho_e = 1,000$ kg/m^3 (water density). We can therefore estimate σ_2 as being equal to 129 MPa. Considering a depth range of 7–9 km and a reasonable 20–30°C/km temperature gradient for the upper continental crust, a mean temperature of 160–230°C is derived, in good agreement with the temperature derived from twin morphology measured in our samples.

Discussion and conclusions

Our structural analyses of the Faryab area reveal that the deformation sequence recorded in the Sargaz complex involved mainly folding and thrusting as a result of progressive deformation related to Cimmerian tectonics. F1 folding developed under conditions of ductile flow related to the underplating of a Devonian–Carboniferous sequence beneath central Iran due to subduction of the Neotethys. The overturned limbs of F_1-folds cut by ductile, thrust shear zones; the metamorphism of these shear zones under lower greenschist-facies conditions indicates a moderate dip upon thrust planes during the Cimmerian orogeny.

Caclite c-axes fabrics in samples1-6 show a symmetric concentration that are normal to foliation. These concentration of c-axes are consistent with contraction component in the convergence systems. Temperature and depth deformation calculated show these fabric are not consistent with F1-folding and green schist metamorphism facies. Samples 7-19 that were collected from thrust shear zone show a post F_1-folding (syn-thrusting) fabric. These fabrics reveal well-oriented calcite grains in a strongly foliated calcschists within the thrust shear zones. In these samples, c-axes fabrics show a asymmetric concentration, is consistent with LT simple shear. This obliquety reveals a strike-slip component on shear plane. These concentration of c-axes in these samples show oblique shearing in thrust shear zones.

Analyses of calcite twins in the Sargaz complex reveal that the maximum compression was oriented NE–SW. The geometric relationship between stress axes and bedding reveals that reconstructed stress systems mainly post-date folding; σ_1 and σ_3 are subhorizontal and σ_2 is subvertical. The ages of the analysed samples, together with the geometric relationship between stress axes and bedding relative to folding and thrusting, indicate that twinning postdates folding and is likely Late Triassic to Early Jurassic in age.

The compressional stress recorded by calcite twinning, along with the style and age of deformation of the Sargaz complex, is likely to be related to subduction of the Neotethys beneath the southern Sanandaj–Sirjan zone, central Iran, by the Middle Triassic. The results of our study demonstrate that a dextral transcurrent regime may have prevailed in metamorphic complexes within the hinterland of the Zagros orogen during Middle Triassic–Jurassic times, related to the oblique subduction of the Neotethys beneath central Iran. Interestingly, Triassic–Early Jurassic σ_1 trends in the Faryab area (hinterland of the Zagros orogen, upper plate) are comparable with Mio–Pliocene σ_1 trends in the Fars province, Zagros Simply Folded Belt (Arabian lower plate) and those recorded upon the southern Iranian Plateau (former Central Iran upper plate; Lacombe et al. 2007). These trends are consistent and oriented NE-SW, in agreement with the present-day compressional trend in the basement below the Hormuz decollement level revealed by earthquake focal mechanisms in the Simply folded belt (Lacombe et al. 2007), which, in the absence of sampling in the stable foreland, supports the absence of larhe thrust sheets rotations in the thrust belt. Although a large time span separates these deformation events, and despite the complexity of the geodynamic setting (i.e., oblique subduction), this similarity could possibly indicate that the two stress regimes in the upper plate remained rather similar to a first-order approximation over the period spanning from the initiation of subduction in the Middle Triassic until the Mio–Pliocene Arabia–Eurasia collision; additional research is clearly required to reach a definitive conclusion regarding this point.

The mean differential stress magnitudes are consistent with values reported previously for the hinterlands of orogens (e.g., Lacombe 2001), and are consistent with a depth of deformation of approximately 7–9 km. The mean width of measured calcite twins documents the occurrence of twinning under a type II twinning regime, which constrains the temperature of deformation to between 170 and 200°C. Patterns of twinning development, including twin type and the depth and temperature of deformation, recorded for samples from the Faryab region are inconsistent with greenschist facies P–T conditions, thereby supporting the proposal that twinning occurred mainly as a late, post-metamorphic deformation event within the tectonic history of the Sargaz complex.

References

Alavi M (1994) Tectonics of the Zagros Orogenic belt of Iran: new data and interpretations. Tectonophysics 229:211–238

Berberian M (1972) Two important deformational and metamorphic phases in the belt northeast of the Zagros thrust line (Iran). Internal Report of the Petrological Department, Geological Survey of Iran, p 13

Berberian M (1973) Two important deformational and metamorphic phases in the belt northeast of the Zagros thrust line (Iran). A brief structural review of the Sanandaj- Sirjan Belt. Geological Survey of Iran, Report No. 27, p 35

Berberian M, Nogol M (1974) Preliminary explanatory text of the geology of DehSard and Khabr maps with some remarks on the metamorphic complex and the tectonics of the area (two 1:100,000 geological sheets from the Hajiabad Quadrangle map). Geological Survey of Iran, Internal Report, p 60, 24 figures, 2 geological maps

Berberian M (1976) An explanatory note on the first Seismotectonic Map of Iran: a seismotectonic review of the country. Geological Survey of Iran, Internal Report No. 39, pp 7–142, 53 Figures, 5 maps

Berberian M, King GC (1981) Toward a paleogeography and tectonic evolution of Iran. Can J Earth Sci 18:210–265

Burkhard M (1993) Calcite twins, their geometry, appearance and significance as stress-strain markers and indicators of tectonic regime: a review. J Struct Geol 15:351–368

Craddock JP, Jackson M, Van Der Pluijm B, Versical RT (1993) Regional shortening fabrics in eastern North America: far-field stress transmission from the Appalachian-Ouachita orogenic belt. Tectonics 12:257–264

Eftekharnejad J (1981) Tectonic division of Iran with respect to sedimentary basins. J Iran Petroleum Soc 82:19–28 (in Farsi)

Evans MA, Groshong RH Jr (1994) A computer program for the calcite strain gauge technique. J Struct Geol 16:277–281

Falcon NL (1967) The geology of north-east margin of the Arabian basement shield. Adv Sci 24:31–42

Ferrill DA (1991) Calcite twin width and intensities as metamorphic indicators in natural low-temperature deformation of limestone. J Struct Geol 13:667–675

Ferrill DA (1998) Critical re-evaluation of differential stress estimates for calcite twins in coarse-grained limestone. Tectonophysics 285:77–86

Ferrill DA, Morris AP, Evans M, Burkhard M, Groshong RH Jr, Onasch CM (2004) Calcite twin morphology: a low-temperature deformation geothermometer. J Struct Geol 26:1521–1529

Friedman M, Teufel LW, Mores JD (1976) Strain and stress analysis from calcite twin lamellae in experimental buckles and faulted drape folds. Philos Trans R Soc Lond, Ser A 283:87–107

Ghasemi H (2001) Petrology, geochemistry and origin of ore deposits in ultramafic and mafic complex of Sikhoran. SE of Iran. Unpublished Ph.D Thesis. University of Tarbiat Modares. Tehran, Iran

Ghasemi A, Talbot CJ (2006) A new tectonic scenario for the Sanandaj-Sirjan zone (Iran). J Asian Earth Sci 26:683–693

Gonzales-Casado JM, Garcia-Cuevas C (1999) Calcite twins from microveins as indicators of deformation history. J Struct Geol 21:875–889

Groshong RH Jr (1972) Strain calculated from twinning in calcite. Bull Geol Soc Am 82:2025–2038

Groshong RH Jr, Pfiffner OA, Pringle LR (1984) Strain partitioning in the Helvetic thrust belt of eastern Switzerland from the leading edge to the internal zone. J Struct Geol 6:5–18

Hushmandzadeh A, Sabzehi M, Breberian M (1972) A brief note on Early Kimmerian orogeny and high grade metamorphism in the Sanandaj-sirjan Belt (Sirjan-Esfandagheh). Geological Survey of Iran, Internal Report, p 30

Jaeger JC, Cook NGW (1969) Fundamentals of rock mechanics. Chapman and Hall, New York, p 585

Jamison WR, Spang JH (1976) Use of calcite twin lamellae to infer differential stress. Geol Soc Am Bull 87:868–872

Lacombe O (2001) Paleostress magnitudes associated with development of mountain belt: Insights from tectonic analyses of calcite twin in the Taiwan Foothills. Tectonics 20:834–849

Lacombe O (2007) Comparison of paleostress magnitudes from calcite twins with contemporary stress magnitudes and frictional sliding criteria in the continental crust: mechanical implications. J Struct Geol 29:86–99

Lacombe O, Laurent P (1992) Determination of principal stress magnitudes using calcite twins and rock mechanics data. Tectonophysics 202:83–93

Lacombe O, Laurent P (1996) Determination of deviatoric stress tensors based on inversion of calcite twin data from experimentally deformed monophase samples: preliminary results. Tectonophysics 255:189–202

Lacombe O, Angelier J, Laurent P (1993) Les macles de la calcite, marqueurs des compressions récentes dans un orogène actif: L'exemple des calcaires récifaux du sud de Taiwan. CR Acad Sci Ser II 316:1805–1813 (in French with abridged English version)

Lacombe O, Amrouch K, Mouthereau F, Dissez L (2007) Calcite twinning constraints on late Neogene stress patterns and deformation mechanisms in the active Zagros collision belt. Geology 35:263–266

Lafrance B (1994) Natural calcite *c*-axis fabric: an alternate interpretation. Tectonophysics 229:1–18

Laurent P, Bernard P, Vasseur G, Etchecopar A (1981) Stress tensor determination from the study of e twins in calcite: a linear programming method. Tectonophysics 78:651–660

Laurent P, Tourneret C, Laborde O (1990) Determining deviatoric stress tensors from calcite twins: application to monophased synthetic and natural polycrystals. Tectonics 9:379–389

Laurent P, Kern H, Lacombe O (2000) Determination of deviatoric stress tensors based on inversion of calcite twin data from experimentally deformed monophase samples, part II. Uniaxial and triaxial stress experiments. Tectonophysics 327:131–148

Majidi B (1972) Preliminary report of the Hadjiabad Quadrangle. Geological Survey of Iran, Internal Report, No.25, p 150

Majidi B (1974) Metamorphic problems of south Iran. Memoirs of the Faculty of Engineering No. 28, Tehran University, pp 120–145

Mohajjel M, Fergusson CL (2000) Dextral transpression in late cretaceous continental collision, Sanandaj-Sirjan Zone, western Iran. J Struct Geol 22:1125–1139

Mohajjel M, Fergusson CL, Sahandi MR (2003) Cretaceous-Tertiary convergence and continental collision, Sanandaj-Sirjan Zone, western Iran. J Asian Earth Sci 21:397–412

Newman J (1994) The influence of grain size and grain size distribution on methods for estimating paleostress from twinning in carbonates. J Struct Geol 16:1589–1601

Pfiffner OA (1982) Deformation mechanisms and flow regimes in limestones from the Helvetic zone of the Swiss Alps. J Struct Geol 4:429–442

Pfiffner OA, Burkhard M (1987) Determination of the paleo-stress axes orientation from fault, twin and earthquake data. Ann Tecton 1:48–57

Rocher M, Lacombe O, Angelier J, Chen HW (1996) Mechanical twin sets in calcite as markers of recent collisional events in a fold-and-thrust belt: evidence from the reefal limestones of southwestern Taiwan. Tectonics 15:984–996

Rocher M, Lacombe O, Angelier J, Deffontaines B, Verdier F (2000) Cenozoic folding and faulting in the North Pyrenean Foreland (Aquitaine Basin, France): insights from combined structural and paleostress analyses. J Struct Geol 22:627–645

Rowe KJ, Rutter EH (1990) Paleostress estimation using calcite twinning: experimental calibration and application to nature. J Struct Geol 12:1–17

Rutter EH (1995) Experimental study of the influence of stress, temperature and strain on dynamic recrystallization of Carrara marble. J Geophys Res Solid Earth 100(B12):24651–24663

Sabzehi M (1974) Les melanges ophiolitiques de la region d, Esfandagheh, These d, etate. Universite Scientifique et Medicale de de Grenoble, France, p 306

Sabzehi M, Berberian M (1972) Preliminary note on the structural and metamorphic history of the area between Dolatabad and Esfandagheh, southern central Iran. Geological Survey of Iran, Internal Report. No. 45., p 150

Sarkarinejad Kh, Azizi A (2008) Slip partitioning and inclined dextral transpression along the Zagros Thrust System, Iran. J Struct Geol 30:116–136

Sarkarinejad KH, Faghih A, Grasemann B (2008) Transpressional deformations within the Sanandaj–Sirjan metamorphic belt (Zagros Mountains, Iran). J Struct Geol 30:818–826

Schroder JW (1944) Essai sur la structure de l'Iran. Ecolage Geologicae Helvetiae 37:37–81

Sengor AMC, Altmer D, Cin A, Ustaomer T, Hsu KJ (1988) Origin and assembly of the Tethyside orogenic collage at the expense of Gondwana land. In: Audley-Charles MG, Hallam A (eds) Gondwana and tethys. Geological Society of London, Special Publication 37, pp 119–181

Shafiei SH (2007) Structural analysis of metamorphic rocks in the Faryab area (south of Esfandagheh), SE Iran. Unpublished Ph.D. Thesis, University of Shahid Beheshti, Tehran, Iran, p 129

Sheikholeslami MR, Pique A, Mobayen P, Sabzehi M, Bellon H, Hashem Emami M (2008) Tectono-metamorphic evolution of the Neyriz metamorphic complex, Quri-kor-e-sefid area (Sanandaj-Sirjan Zone, SW Iran). J Asian Earth Sci 31:504–521

Shelly D (1989) Calcstress: a program that calculates compression and tension direction from calcite U-stage data. Comp Geosci 11:269–273

Spang JH (1972) Numerical method for dynamic analysis of calcite twin lamellae. Geol Soc Am Bull 83:467–472

Stocklin J (1968) Structural history and tectonics of Iran: a review. Am Assoc Pet Geol 52(7):1229–1258

Townend J, Zoback MD (2000) How faulting keeps the crust strong. Geology 28(5):399–402

Tullis TE (1980) The use of mechanical twinning in minerals as a measure of shear stress magnitude. J Geophys Res 85:6263–6268

Turner FJ (1953) Nature and dynamic interpretation of deformation lamellae in calcite of three marbles. Am J Sci 251:276–298

Turner FJ (1962) Compression and tension axes determined from [0112] twinning in calcite. J Geophys Res 67:1660

Turner FJ, Weiss LE (1963) Structural analysis of metamorphic tectonites. McGraw-Hill, New York, p 545

van der Pluijm BA, Craddock JP, Graham BR, Harris JH (1997) Paleostress in cratonic north America: implications for deformation of continental interiors. Science 277:794–796

Watters WA, Sabzehi M (1970) Preliminary report, geology and topography of the metamorphic and igneous complex of the central part of the Neyriz Quadrangle. Geological Survey of Iran, Internal Report, p 130

Weiss LE (1954) A study of tectonic style: structural investigation of a marble quartzite complex in southern California. Geol Sci Univ Calif Publ 30:1–102

Wenk HR, Takeshita T, Bechler E, Erskine BG, Matties S (1987) Pure shear and simple shear calcite textures. Comparison of experimental, theoretical and natural data. J Struct Geol 9:731–745